Laboratory Investigation (2015) 95, 962–972

Transcriptional upregulation of HNF-1β by NF-κB in ovarian clear cell carcinoma modulates susceptibility to apoptosis through alteration in bcl-2 expression

Erina Suzuki, Sabine Kajita, Hiroyuki Takahashi, Toshihide Matsumoto, Tomoko Tsuruta and Makoto Saegusa

Hepatocyte nuclear factor-1β (HNF-1β) is a transcriptional factor that has an important role in endometriosis–ovarian clear cell carcinoma (OCCC) sequence by modulating cell kinetics and glucose metabolism. However, little is known about the detailed molecular mechanisms that govern its regulation and function. Herein, we focus on upstream and downstream regulatory factors of HNF-1β in OCCCs. In clinical samples, HNF-1β expression was positively correlated with the active form of NF-κB/p65 in OCCCs, and closely linked with a low nuclear grade and non-solid architecture. In cell lines, transfection of p65 resulted in increased HNF-1β mRNA and protein expression in TOV-21G cells (OCCC cell line with endogenous HNF-1β expression), in line with activation of the promoter, probably through interacting with the basic transcriptional machinery. Suppression of endogenous HNF-1β expression by siRNA increased apoptosis in TOV-21G cells, while treatment of Hec251 cells (endometrial carcinoma cell line with extremely low endogenous HNF-1β expression) stably overexpressing exogenous HNF-1β with doxorubicin abrogated apoptosis of the cells, along with increased ratio of bcl-2 relative to bax. Moreover, overexpression of HNF-1β led to upregulation of bcl-2 expression at the transcriptional level in TOV-21G cells, which provided evidence for a positive correlation between HNF-1β and bcl-2 expression in OCCCs. These data, therefore, suggest that association between HNF-1β and NF-κB signaling may participate in cell survival by alteration of apoptotic events, particularly in mitochondria-mediated pathways, through upregulation of bcl-2 expression in OCCCs.

Laboratory Investigation (2015) **95,** 962–972; doi:10.1038/labinvest.2015.73; published online 1 June 2015

Epithelial ovarian carcinomas, consisting of four histologically distinct subtypes, including serous, mucinous, endometrioid, and clear cell types, have the worst prognosis of all gynecological malignancies.[1] Of these, ovarian clear cell carcinomas (OCCCs) are not just another type of epithelial ovarian carcinoma, but a distinct entity with a specific carcinogenic mechanism.[2] For example, OCCCs often show chemoresistance and are accompanied by thromboembolic complication. The clinical outcome in the advanced stage is generally unfavorable, despite their slow growth.[3–5] In addition, they are frequently associated with endometriosis, which is thought to be a precursor of tumor lesions.[6,7]

Hepatocyte nuclear factor-1β (HNF-1β) is a homeodomain-containing transcription factor that shares $>80\%$ amino-acid sequence homology with the homeodomain of HNF-1α.[8] HNF-1β and HNF-1α bind to the same DNA sequence as homodimers or heterodimers, and regulate the expression of multiple genes that modulate cell cycle progression, susceptibility to apoptosis, and glucose metabolism through direct or indirect mechanisms.[9–11] Previous studies have revealed that specific expression of HNF-1β, probably due to hypomethylation of the CpG islands in the promoter region, is frequently observed in OCCCs and endometriotic cysts.[12–14]

The high concentration of free iron due to repeated hemorrhage and inflammation is frequently detected in ovarian endometriotic cysts, promoting carcinogenesis through iron-induced persistent oxidative stress and DNA damage.[11,15] Interestingly, iron-induced reactive oxygen species (ROS) signaling participates in endometriotic cell survival possibly by acting in detoxification and anti-apoptotic pathways through overexpression of HNF-1β.[16,17] However, little is known about the association between HNF-1β expression and inflammatory cytokines, such as NF-κB, in the

Department of Pathology, Kitasato University School of Medicine, 1-15-1 Kitasato, Minami-ku, Sagamihara, Japan
Correspondence: Professor M Saegusa, M.D, Department of Pathology, Kitasato University School of Medicine, 1-15-1 Kitasato, Minami-ku, Sagamihara, Kanagawa 252-0374, Japan.
E-mail: msaegusa@med.kitasato-u.ac.jp

Received 22 December 2014; revised 8 April 2015; accepted 21 April 2015

endometriosis–OCCC sequence. Moreover, the detailed mechanisms that govern HNF-1β-mediated modulation of cell kinetics, including cell proliferation and apoptosis, in OCCCs remain to be clarified. We therefore extensively investigated HNF-1β expression, together with examination of NF-κB signaling and apoptotic pathways, as well as expression of its related molecules, including HNF-4α and Glut-1, in OCCCs and endometriotic cysts.

MATERIALS AND METHODS

Clinical Cases

A total of 94 cases of OCCCs, surgically resected at Kitasato University Hospital in the period from 2002 to 2012, were selected from our patient records, according to the criteria of the 2003 World Health Organization classification. The mean age of the patients was 54.8 years (range, 33–75 years). Sixty cases were subcategorized as stage I and 34 as stage II to IV, according to the criteria of the International Federation of Gynecology and Obstetrics (FIGO),[18] and 8 were positive for nodal metastasis whereas 70 were negative.

Tumors were graded based on the nuclear features, as described by Veras *et al*[19] with minor modifications, as follows: nuclear grade (NG) 1, small round nuclei with smooth nuclear contours and small nucleoli; NG2, enlarged nuclei with some enlarged nucleoli; and NG3, highly pleomorphic nuclei with vesicular chromatin and prominent nucleoli. Tumor architecture was also subdivided into two categories, solid and non-solid patterns, the latter including papillary and tubulocystic features (Figure 1). The nuclear grade and architecture were determined based on the highest grade or feature providing it comprised at least 30% of the tumor. Tumors were further subdivided into three groups on the basis of a combination of nuclear grade and growth architecture, as follows: group A, NG1 and non-solid; group B, NG1-solid, NG2-solid or -non-solid, and NG3-non-solid; and group C, NG3-solid.

Thirty-nine endometriotic and 19 atypical endometriotic cysts were also selected, according to the criteria described by Versa *et al*.[19] In addition, 10 cases of endometrioid, 10 of mucinous, and 10 of serous adenocarcinomas were also evaluated.

All tissues were routinely fixed in 10% formalin and processed for embedding in paraffin wax. Approval for this study was given by the Ethics Committee of the Kitasato University School of Medicine (B12-58).

Antibodies and Reagents

Anti-HNF-1β, anti-NF-κB/p65, anti-HIF-1α, anti-p27^{kip1}, anti-Rb, and anti-bax antibodies were purchased from BD Biosciences (San Jose, CA, USA). Anti-HNF-4α and

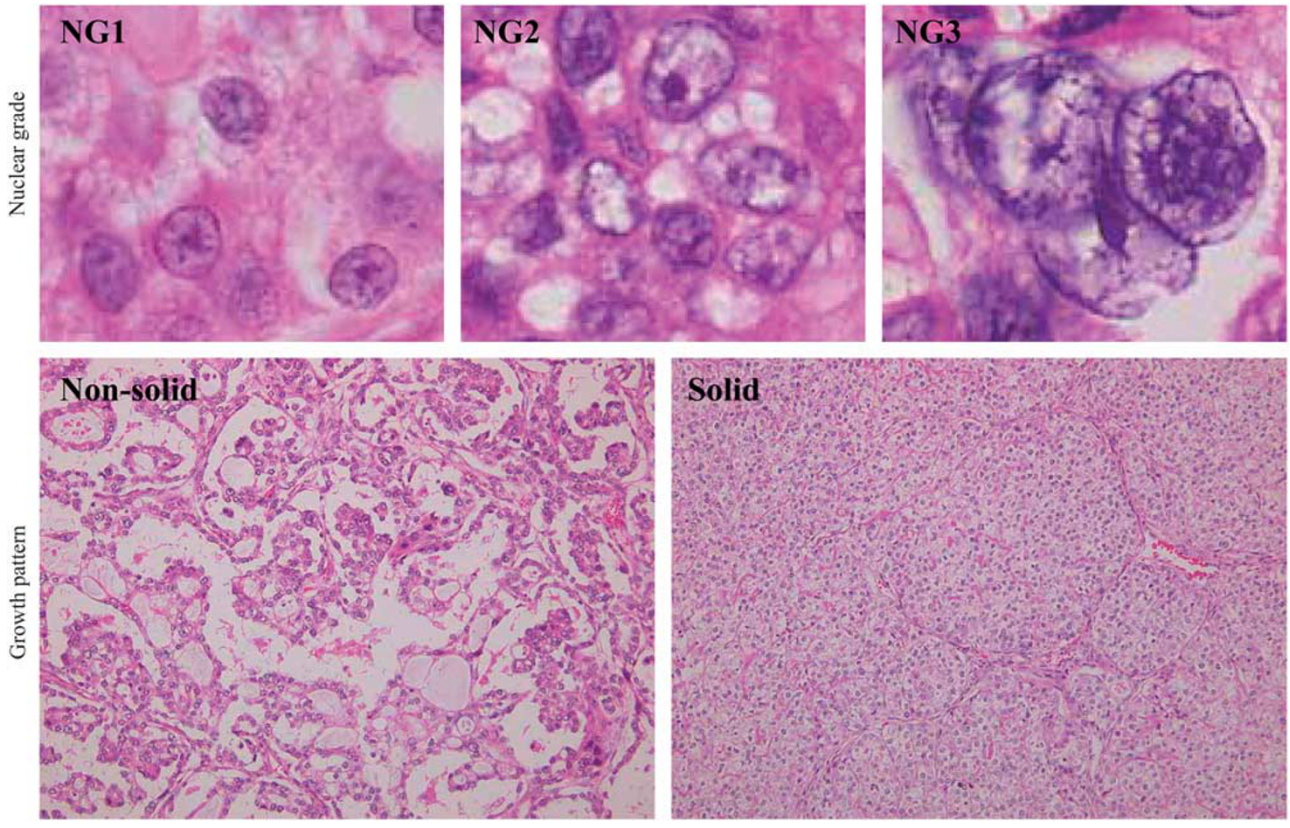

Figure 1 Nuclear grade and tumor growth pattern in ovarian clear cell carcinomas (OCCCs). Upper: nuclear grade (NG)1 (right), NG2 (middle), and NG3 (left). Original magnification, ×400. Lower: tumor growth patterns: non-solid (left) and solid features (right). Original magnification, ×100.

anti-β-actin antibodies were bought from Sigma-Aldrich Chemicals (St Louis, MO, USA). Anti-phospho-p65 at Ser275 (pp65), anti-phospho-Rb at Ser807/811 (pRb), and anti-cleaved caspase 3 antibodies were obtained from Cell Signaling Technology (Danvers, MA, USA). Anti-bcl-2, anti-$p21^{waf1}$, anti-cyclin D1, and anti-Ki-67 antibodies were purchased from Dako (Copenhagen, Denmark). Anti-Glut-1 and anti-survivin antibodies were bought from Millipore (Billerica, MA, USA) and R&D Systems (Minneapolis, MN, USA), respectively. Anti-HA antibody was obtained from Santa Cruz Biotechnology (Santa Cruz, CA, USA). TNF-α, cisplatin, and doxorubicin were purchased from Sigma.

Immunohistochemistry (IHC)

IHC was performed using a combination of the microwave-oven heating and polymer immunocomplex (Envision, Dako) methods.

For evaluation of IHC findings, scoring of nuclear or cytoplasmic immunoreactivity for HNF-1β, pp65, HNF-4α, HIF-1α, and Glut-1 was performed, as described previously.[20,21] Briefly, the proportion of immunopositive cells among the total number of counted cells was subdivided into five categories as follows: 0, all negative; 1, <10%; 2, 10–30%; 3, 30–50%; and 4, >50% positive cells. The immunointensity was also subclassified into four groups: 0, negative; 1, weak; 2, moderate; and 3, strong immunointensity. IHC scores were generated by multiplication of the values of the two parameters. Nuclear immunopositivity for Ki-67 was also counted in at least 1000 cells in five randomly selected fields. Labeling indices (LIs) were then calculated as number per 100 cells, as described previously.[20,21]

Apoptosis and TUNEL (TdT-Mediated dUTP-Biotin Nick-End Labeling) Assay

Apoptotic cells were identified in HE-stained sections, according to the criteria of Kerr *et al.*[22] A total of 20 fields were randomly selected, and the amount of apoptotic cells was calculated by counting the mean number of apoptotic figures per 10 high power fields.

The *In Situ* Cell Death Detection Kit (Roche, Tokyo, Japan) was also used for detection of apoptotic cells, according to the manufacturer's instructions. The number of positive cells was counted among at least 700 cells, and apoptotic LIs were then calculated as number per 100 cells.

Plasmids and Cell Lines

Full-length cDNA for human HNF-1β (Open Biosystems, Huntsville, AL, USA) with or without HA tag was subcloned into pcDNA3.1 (Invitrogen, Carlsbad, CA, USA). The *HNF-1β* promoter sequence between –1470 and either +47 or +216 base pair (bp) relative to the transcription start site (NG013019) was amplified by PCR and subcloned into the pGL3-basic vector (Promega, Madison WI, USA). A series of 5′-truncated constructs were generated by PCR- and enzyme digestion-based methods. The *bcl-2* promoter region between −1650 and −67 bp relative to the translation start site (EU119400), and the *Glut-1* promoter between −2057 and either +18 or +425 bp relative to the transcription start site (NG008232) were also amplified, and a series of 5′-truncated constructs were generated using similar procedures. In the latter, site-directed mutagenesis of a putative HNF-1β binding site in the promoter was performed using the PrimeSTAR Mutagenesis Basal kit (Takara Bio, Shiga, Japan). The identity of all constructs was confirmed by sequencing prior to use. The sequences of PCR primers employed in this study are listed in Table 1. In addition, the pGL4B-HNF-4α reporter construct was obtained from the Riken DNA Bank Human Resource (Tsukuba, Ibaragi, Japan). The pGL3B–survivin–luc and the pcDNA-3.1 mouse p65 expression vectors were used as described previously.[21,23]

The TOV-21G cell line was obtained from the American Type Culture Collection (Manassas, VA, USA), and OVISE, OVTOKO, Hec251 cells were from the National Institute of Biomedical Innovation (Osaka, Japan). To establish

Table 1 Primer sequences used in this study

Gene			Sequence
HNF-1β	Promoter	(−1470) Forward	5′-AACTGGCTTCCCGTCTTCTCAG-3′
		(−140) Forward	5′-AGTACAATGGACCCTGGCAAAG-3′
		(−14) Forward	5′-ACCATCATTTGCATCCAGCCGA-3′
		(+216) Reverse	5′-AAGGACGGAAAAAGAAGGGGGT-3′
		(+47) Reverse	5′-CTAACTTGCCATGATCGCCACC-3′
	mRNA	(187) Forward	5′-AAATGGTGTCCAAGCTCACGT-3′
		(388) Reverse	5′-TTGGTGAGAGTATGGAAGACC-3′
	ChIP	E1 forward	5′-GGAGTAACAGGTGTCTGGAGG-3′
		E1 reverse	5′-GTGCGAGAGAGGAGGGTGGA-3′
		E2 forward	5′-AGTTGCCGGGACTACAGGCG-3′
		E2 reverse	5′-ACCATCCTGGCTAACACAGT-3′
bcl-2	Promoter	(−1650) Forward	5′-CCTTTAACCCGGGCCAGGGA-3′
		(−429) Forward	5′-GTAAATTTAATTTCCAGGCA-3′
		(−229) Forward	5′-AATAATAACGTGCCTCATGA-3′
		(−160) Forward	5′-AAGTGTTCCGCGTGATTGAA-3′
		(−67) Reverse	5′-CCCAGAGAAAGAAGAGGAGT-3′
	mRNA	(382) Forward	5′-TGGGAAGGATGGCGCACG-3′
		(820) Reverse	5′-CAGTTCACCCCGTCCCTG-3′
Glut-1	Promoter	(−2057) Forward	5′-TGGAAGTATCAGCAGGACGGACT-3′
		(−255) Forward	5′-AGGGAAGGGAGAAGTCAATC-3′
		(−63) Forward	5′-TCCAGTCCAGCTTTCCACC-3′
		(+425) Reverse	5′-ACTCCCACTGCGACTCTGA-3′
		(+18) Reverse	5′-TCTCTAGCAAAATGGTGGAGCCG-3′
	mRNA	(1711) Forward	5′-AGCCAGGGTCCACGTCCAGCT-3′
		(2011) Reverse	5′-GGGCGACTCACACTTGGGAATC-3′

Hec251 cells that stably overexpress HA-HNF-1β, cells were transfected with the expression plasmid or empty vector, and stable clones were established, as described previously.[20,21]

Transfection

Transfection of vectors was carried out using LipofectAMINE PLUS (Invitrogen), and luciferase activity was assayed, as described previously.[20,21] The two siRNAs for HNF-1β or the negative control were transfected using the siPORT NeoFX transfection agent (Ambion, Austin, TX, USA), according to the manufacturers' instructions.

RT-PCR (Reverse Transcription-PCR)

cDNA was synthesized from 2 μg of total RNA. Amplification was carried out in the exponential phase to allow comparison among cDNAs synthesized from identical reactions, using specific primers (Table 1). Primers for the *GAPDH* gene were also applied, as described previously.[20,21] For quantitative analysis, real-time PCR was carried out using a Power SYBR Green PCR Master Mix (Applied Biosystems, Foster City, CA, USA). Fluorescent signals were detected using the ABI 7500 real-time PCR System and data were analyzed using the associated ABI 7500 System SDS Software (Applied Biosystems).

Chromatin Immunoprecipitation (ChIP) Assay

ChIP analysis was performed using an EpiXplore ChIP assay kit (Clontech Laboratory, Mountain View, CA, USA). Briefly, after transfection with the p65 vector, the cells were cross-linked with formaldehyde. Cell lysates were sonicated to shear the DNA to a length between 200 and 1000 bp, and were then precipitated overnight using an anti-NF-κB/p65 antibody or mouse IgG as negative control, along with magnetic beads. After proteinase K digestion, the DNA was extracted and analyzed by 25 to 30 cycles of PCR. ChIP analysis was conducted, using two specific primer sets (Table 1).

Western Blot Assays

Total cellular proteins were isolated using RIPA buffer (50 mmol/l, Tris-HCL (pH7.2), 1% Nonidet P-40, 0.5% sodium deoxycholate, 0.1% sodium dodecyl sulfate). Nuclear and cytoplasmic fractions were prepared using NE-PER Nuclear and Cytoplasmic Extraction Reagents (Pierce Biotechnology, Rockford, IL, USA). Aliquots of the proteins were resolved by SDS-PAGE, transferred to membranes, and probed with primary antibodies, coupled with the ECL detection system (Amersham Pharmacia Biotechnology, Tokyo, Japan). The intensity of individual signals was measured with the ImageJ software version 1.41 (NIH, Bethesda, MD, USA), as detailed earlier.[20,21]

Flow Cytometry

For cell cycle analysis, cells were fixed using 70% alcohol and stained with propidium iodide (Sigma). The prepared cells were analyzed by flow cytometry using BD FACS Calibur and the associated CellQuest Pro software (BD Biosciences).

Statistics

Comparative data were analyzed using the Mann–Whitney *U*-test, χ^2- test, and the Pearson's correlation coefficient, whichever was appropriate. The cutoff for statistical significance was set as $P<0.05$.

RESULTS

Expression of HNF-1β and Its Related Molecules in OCCCs and Endometriotic Cysts

Representative IHC findings for HNF-1β and its related molecules in OCCCs and ovarian endometriotic cysts are illustrated in Figure 2. Distinct nuclear immunostaining for HNF-1β, pp65, HNF-4α, HIF-1α, and Ki-67 was mainly observed in epithelial cells, whereas cytoplasmic immunoreaction for Glut-1 was evident in both epithelial cells and erythrocytes.

Average IHC scores for HNF-1β and pp65 were significantly higher in atypical endometriotic cysts and NG1 OCCCs than those in endometriotic cysts and NG3 tumors, whereas HNF-4α and Glut-1 scores and Ki-67 LIs showed stepwise increase from endometriotic cysts through NG1 to NG3 tumors (Figure 3a). In addition, HNF-1β and pp65 scores were also significantly higher in OCCCs with non-solid pattern than solid pattern, in contrast to significantly higher Glut-1 scores and Ki-67 LIs in the latter (Figure 3b). A combination of NG and growth pattern revealed that HNF-1β and pp65 scores were significantly higher in group A (NG1-non-solid) than those in group C (NG3-solid), in contrast to HNF-4α and Glut-1 scores and Ki-67 LIs (Figure 3c). Significant association between nuclear grade and growth pattern was observed in OCCCs (Supplementary Table S1), whereas clinicopathological factors, such as clinical stage and lymph node status, were not linked with any of the IHC markers, or the two histological features (Supplementary Table S2).

Average HNF-1β scores were positively correlated with only pp65 scores in OCCCs. Similar findings were also observed in endometriotic cysts, with the exception of the inverse correlation with Ki-67 LIs (Supplementary Tables S3 and S4).

With regard to associations with histological subtypes of ovarian carcinomas, HNF-1 β and pp65 scores were significantly higher in OCCCs as compared with the other subtypes, in contrast to significantly higher HNF-4α scores in the mucinous type (Supplementary Figure S1).

Transcriptional Upregulation of HNF-1β by NF-κB/p65

On the basis of the above IHC findings, we examined an association between HNF-1β and NF-κB signaling, using TOV-21G and Hec251 cells treated with TNF-α, known as an activator of NF-κB signaling.[24–26] In TOV-21G cells, although short-term exposure to TNF-α resulted in upregulation of

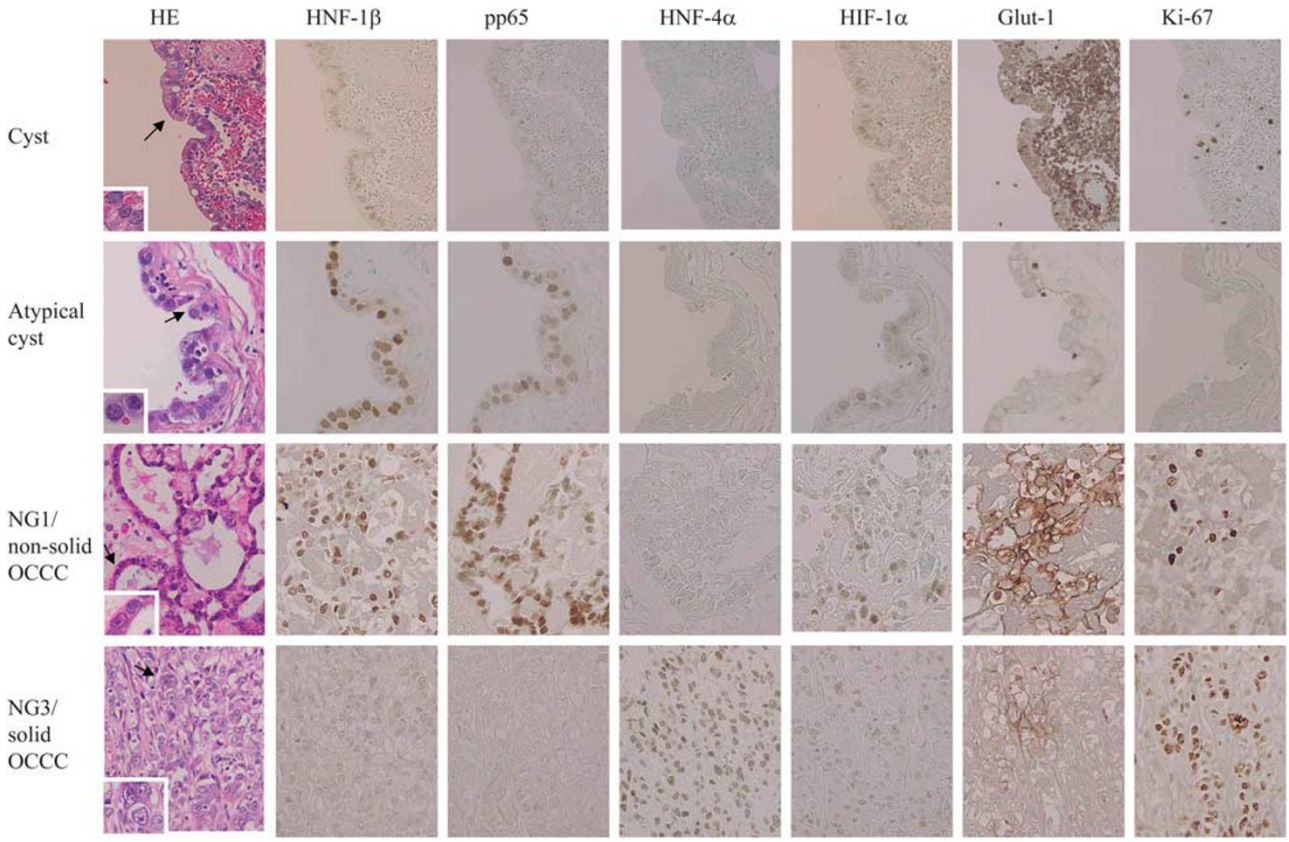

Figure 2 Immunohistochemistry (IHC) findings in serial sections of ovarian endometriotic cysts with or without atypia and ovarian clear cell carcinomas (OCCCs). Staining is by hematoxylin and eosin (HE) and by IHC for HNF-1*β*, pp65, HNF-4*α*, HIF-1*α*, Glut-1, and Ki-67 in ovarian endometriotic cysts (Cyst), atypical endometriotic cysts (Atypical cyst), and OCCCs. Note the nuclear features (indicated by arrows and magnified in the insets) in cystic and tumor lesions. Original magnification, ×200 and ×400 (inset).

HNF-1*β* mRNA expression within 1 h, changes in the protein expression level were relatively minor, probably owing to a high level of the endogenous protein. In the treatment of Hec251 cells with extremely low endogenous HNF-1*β* expression, short-term exposure to TNF-*α* caused an increase in HNF-1*β* mRNA levels within 0.5 h, whereas the nuclear level of HNF-1*β* protein transiently increased within 1 h (Figure 4a).

To examine whether NF-κB signaling contributed to transcriptional regulation of HNF-1*β* expression, transient transfection was carried out using TOV-21G. As shown in Figure 4b, transfection of p65 caused increased HNF-1*β* mRNA and protein expression, in line with activation of the promoter in a dose-dependent manner. We noticed that a 1517-bp fragment upstream of the transcription start site in the *HNF-1β* gene contained two potential binding sites of NF-κB, on the basis of a consensus NF-κB binding sequence 5′-GGRNNYYCC-3′ (Figure 4c). However, the shortest construct, which lacks both putative binding sites, still preserved the responsiveness to p65 transfection (Figure 4d). Finally, ChIP assay revealed that transfected p65 promoted its own recruitment to the proximal region between +89 and +179 bp within the promoter (Figure 4e).

Relationship of HNF-1β with Apoptosis, Cell Proliferation, and bcl-2 Expression

Previous studies have demonstrated that HNF-1*β* is essential for the survival of OCCC cells.[9–11] To determine if there is a correlation between expression of HNF-1*β* and apoptosis, we first evaluated clinical samples. Apoptotic cells were readily detected in HE-stained sections on the basis of characteristic features,[22] and the values were positively correlated with apoptotic LIs as detected by the TUNEL assay (Figure 5a). The average amount of apoptotic cells was significantly higher in NG1, non-solid, and group A categories in OCCCs (Figure 5b), but no significant correlation with HNF-1*β* score was observed (Supplementary Tables S3 and S4).

Investigation into whether induction of apoptosis was affected by HNF-1*β* as well as the mechanisms involved was carried out by performance of *in vitro* assays. Following suppression of endogenous HNF-1*β* by transfection of siRNAs into TOV-21G cells (Figure 6a), the amount of apoptotic cells was significantly increased within 48 h, despite no alteration in the expression of survivin, bcl-2, and bax (Figure 6b). Treatment of TOV-21G cells with cisplatin caused an increase in the amount of apoptotic cells, as well as expression of cleaved caspase 3, in a dose-dependent manner,

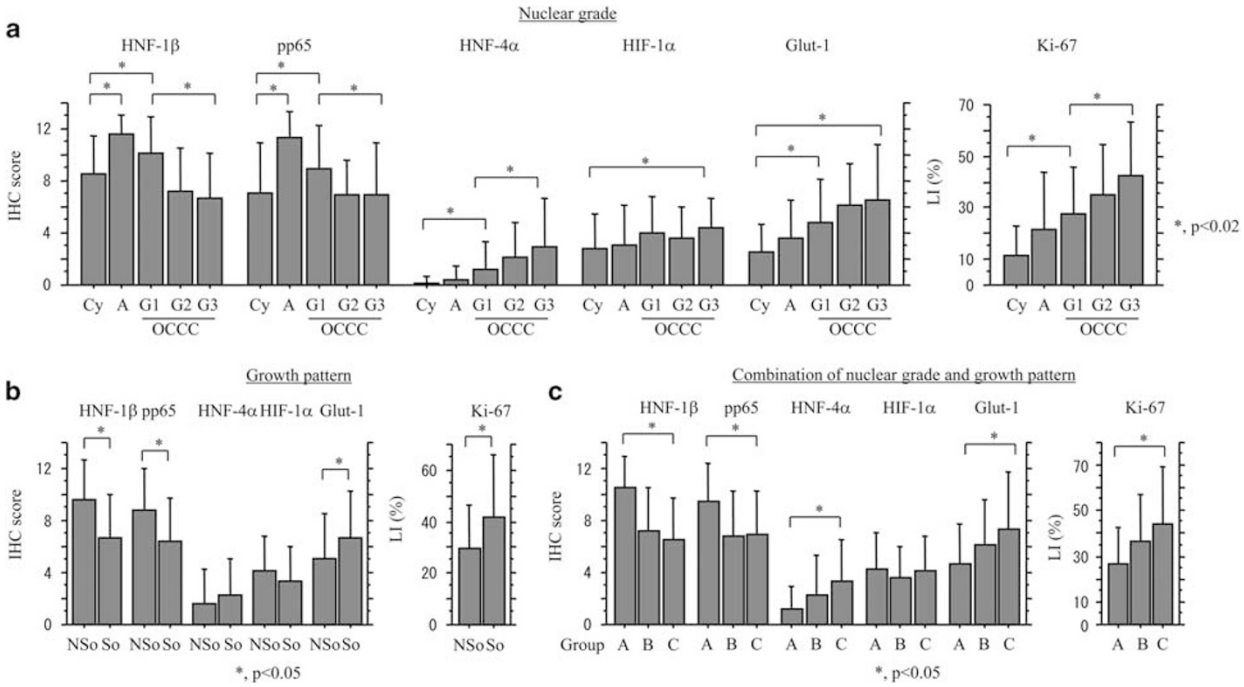

Figure 3 Relationship of the immunohistochemistry (IHC) markers with nuclear grade and growth pattern in ovarian clear cell carcinomas (OCCCs). (**a**) Relation between nuclear grade and IHC scores (left), as well as Ki-67 labeling indices (LIs) (right). Cy, endometriotic cyst; A, atypical endometriotic cyst; G, nuclear grade. (**b**) Relation between tumor growth patterns and IHC scores (left), as well as Ki-67 LIs (right). NSo, non-solid pattern; So, solid pattern. (**c**) Relation of a combination of nuclear grade and growth patterns with IHC scores (left), as well as Ki-67 LIs (right). The data shown are means ± s.d.

whereas HNF-1β expression was completely abrogated by higher, but not lower, doses of cisplatin (Supplementary Figure S2). Moreover, suppression of endogenous HNF-1β expression resulted in an enhancement of cisplatin-induced apoptosis, along with alterations in bcl-2 and bax expression (Figure 6c).

To further examine whether overexpression of HNF-1β affected apoptosis, two independent cell lines stably overexpressing exogenous HNF-1β were established. Treatment of the stable cells with doxorubicin resulted in a reduction in the quantity of apoptotic cells and stabilization of exogenous HNF-1β, along with increases in the relative ratios of bcl-2 to bax and survivin expression at 48 h as compared with control cells (Figure 7a).

Transfection of HNF-1β resulted in increased promoter activity of *bcl-2* and *HNF-4α*, but not *survivin* (Supplementary Figure S3A). The overexpression was also able to induce bcl-2 mRNA and protein expression. A search of the 1600-bp fragment upstream of the translation start site in the *bcl-2* gene revealed one potential HNF-1β-binding site (ATTAAC). In a series of 5′-truncated promoter constructs, the shortest reporter construct (−167 to − 67 bp), which lacks the putative binding site, still retained the promoter activity (Figure 7b), suggesting an association with the basic transcriptional machinery at the promoter. In OCCCs, immunoreactivity for bcl-2 was significantly associated with NG1, non-solid, and group A categories, and the score was positively correlated with the HNF-1β status (Figure 7c and Supplementary Figure S3B).

To examine whether HNF-1β contributed to changes in cell kinetics, quiescence was induced in the three OCCC cell lines by serum starvation and then restimulated with serum. However, HNF-1β expression was not altered during steady cell growth (Supplementary Figure S4A). The two independent clones of Hec251 cells stably overexpressing HNF-1β also showed no difference in cell proliferation rate as compared with the mock case (Supplementary Figure S4B).

As it is known that HNF-1β has a central role in glucose homeostasis,[9–11] an association between HNF-1β and Glut-1 expression was investigated. Transfection of HNF-1β induced a significant increase in Glut-1 mRNA and protein expression, in line with activation of the promoter (Supplementary Figure S5A). On the basis of the potential HNF-1β-binding site (GTTAAT) in the *Glut-1* promoter, a series of 5′-truncated promoter constructs were generated (Supplementary Figure S5B). Deletion from − 2057 to − 255 bp had little effect on induction of promoter activity by HNF-1β, whereas that from − 225 to − 63 bp did so at only a very low level. An additional promoter construct carrying four nucleotide alterations in the putative HNF-1β-binding site led to considerable reduction in response to HNF-1β (Supplementary Figure S5C), suggesting the region from − 152 to − 147 bp

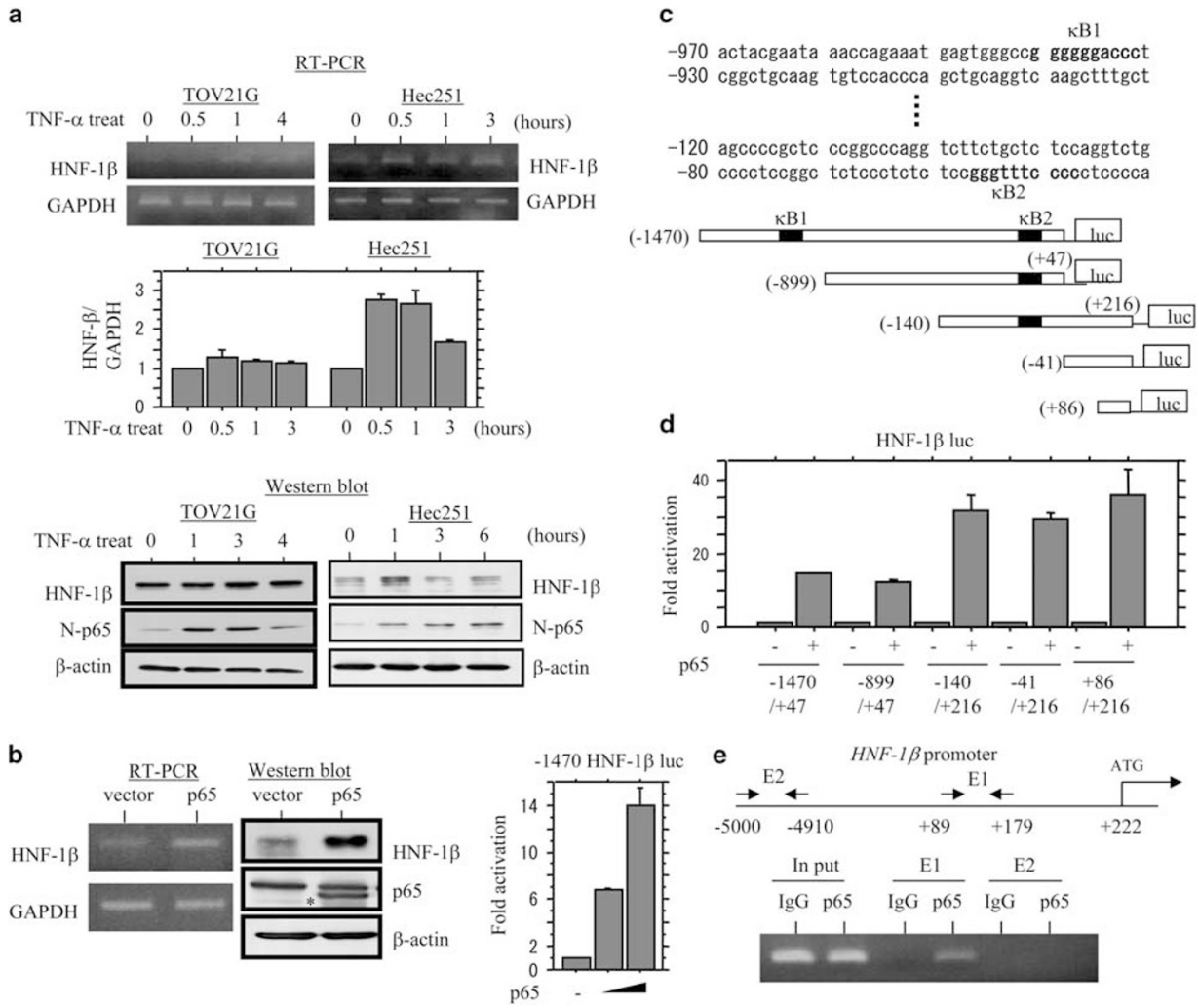

Figure 4 Transcriptional upregulation of HNF-1β by NF-κB/p65. (**a**) Conventional reverse transcription-PCR (RT-PCR; upper) and real-time RT-PCR (middle) analyses of HNF-1β mRNA expression, and western blot analysis (lower) of HNF-1β, as well as nuclear p65 (N-p65), expression in TOV-21G (left) and Hec251 cells (right) for the time shown after exposure to 20 ng/ml TNF-α. (**b**) Left: analyses of mRNA and protein expression levels of *HNF-1β* using total RNA or protein extracted from p65-transfected TOV-21G cells by RT-PCR (left) and western blot assays (right), respectively. Note the exogenous p65 (indicated by asterisk) in the middle panel of the western blot assay. Right: TOV-21G cells were transfected with HNF-1β reporter constructs, together with p65. Relative activity was determined based on arbitrary light units of luciferase activity normalized to pRL-TK activity. The activities of the reporter plus the effector relative to that of the reporter plus empty vector are shown as means ± s.d. The experiment was performed in duplicate. (**c**) Upper: the *HNF-1β* promoter sequence containing two putative NF-κB-binding sites including κB1 and κB2 sites. Lower: various promoter constructs were used for evaluating transcriptional regulation of the *HNF-1β* promoter by p65. (**d**) TOV-21G cells were transfected with various constructs of the *HNF-1β* promoter, along with p65 expression plasmids. The experiment was performed in triplicate. (**e**) Chromatin immunoprecipitation (ChIP) assay data showing that p65 is bound to the proximal (element (E1)), but not distal (E2), region of the *HNF-1β* promoter.

is required for the *Glut-1* promoter to be stimulated by HNF-1β. However, such associations were not observed in OCCCs and endometriotic cysts (Supplementary Tables S3 and S4).

DISCUSSION

Several lines of evidence from the present study support the role of NF-κB/p65 as a transcriptional activator of HNF-1β. First, treatment of Hec251cells with TNF-α caused an increase in HNF-1β mRNA and protein expression, along with nuclear p65 stabilization. Further, transient transfection of p65 led to increased expression of HNF-1β at both mRNA and protein levels. Moreover, p65 could transactivate the *HNF-1β* promoter by binding to the region from −14 to +216 bp of the transcriptional start, probably through interacting with the basic transcriptional machinery at the promoter. Finally, HNF-1β immunoreactivity was positively correlated with the pp65 status in both OCCCs ($r=0.73$, $P<0.0001$) and endometriotic cysts ($r=0.89$, $P<0.0001$).

The environment inside endometriotic cysts is affected by severe oxidative stress.[15] Given that some ROS act as a messenger in the TNF-α- and okadaic acid-induced

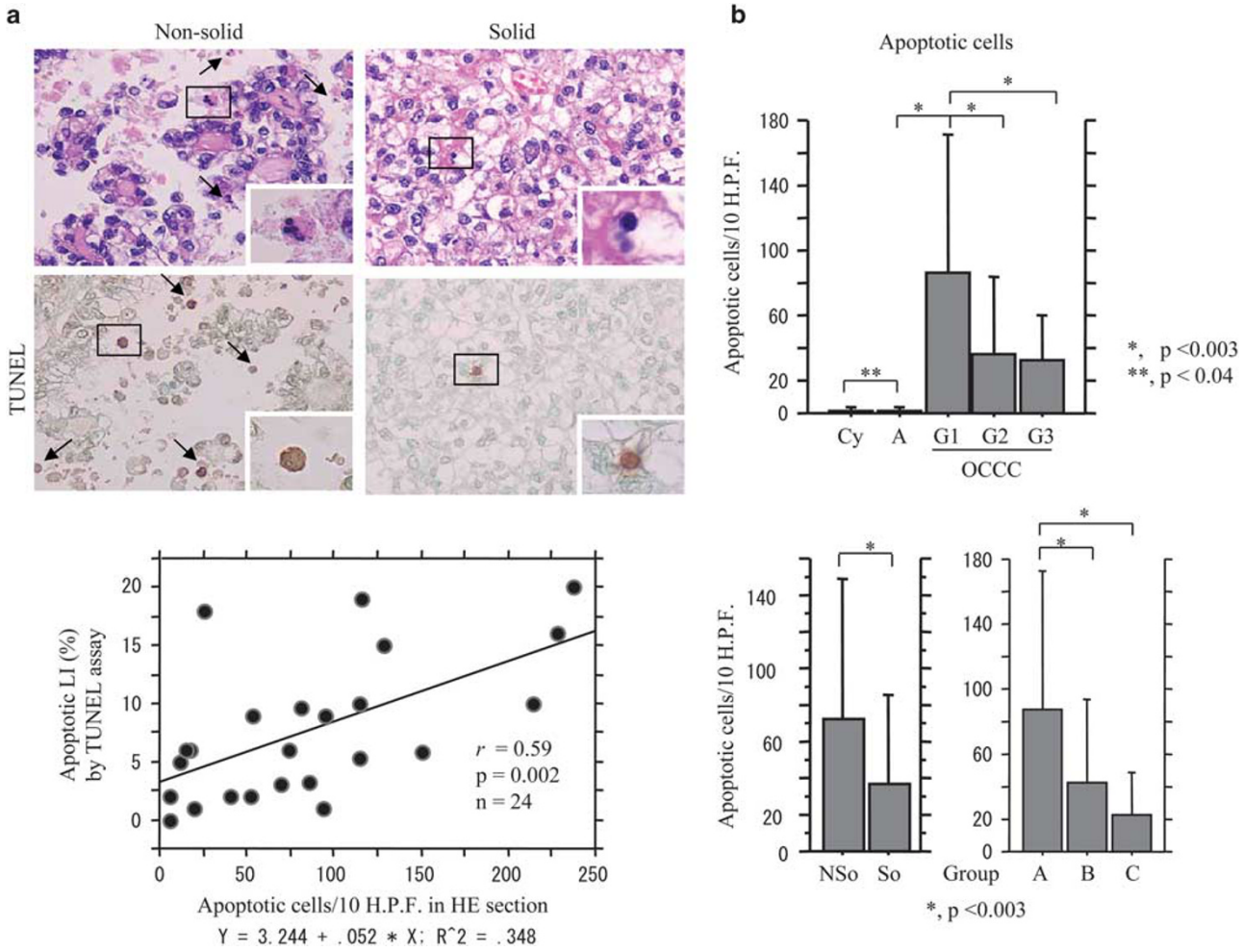

Figure 5 Frequent apoptotic findings in ovarian clear cell carcinomas (OCCCs) with NG1 and non-solid features. (**a**) Upper: detection of apoptotic cells (indicated by arrows) by hematoxylin and eosin (HE) sections (upper) and TUNEL (TdT-Mediated dUTP-Biotin Nick-End Labeling) assay (lower). The enclosed boxes magnified in the insets. Original magnification, ×200 and ×400 (inset). Lower: correlation for detection of apoptotic cells between HE sections and TUNEL assay. (**b**) Upper: apoptotic cells detected by HE sections in endometriotic cysts (Cy), atypical endometriotic cysts (**a**), and OCCCs. G, nuclear grade. Lower: relationship of apoptotic cells detected by HE sections with tumor growth pattern (left) and a combination of nuclear grade and growth patterns (right). The data shown are means ± s.d. NSo, non-solid; So, solid.

post-translational activation of NF-κB/p65,[24] it is suggested that persistent oxidative stress induced by repeated hemorrhage in endometriotic cysts may serve as an activator of NF-κB signaling, and this in turn may cause induction of HNF-1β expression. In fact, our results revealed that high expression levels of pp65, as well as HNF-1β, were observed in endometriotic cysts.

An interest finding in this study was that the HNF-1β score was positively associated with low nuclear grade and non-solid structures in OCCCs with low cell proliferation activity, in contrast to the relatively low scores in tumors that displayed high nuclear grade and solid architecture, as well as high cell proliferation activity. Given that HNF-1β acts as an inducer of potent cell cycle regulatory genes that inhibit G1 progression, including CDKNA1A and CDKN1B,[27] it was expected that HNF-1β may function as a suppressive effector of cell proliferation in OCCCs. Our results, however, demonstrated that HNF-1β expression did not alter during steady cell growth in OCCC cells, as well as in Hec251 cells stably overexpressing exogenous HNF-1β. Moreover, HNF-1β score showed a weak negative correlation ($r = -0.35$, $P = 0.001$) with Ki-67 LIs in OCCCs, indicating that this molecule may be simply associated with less aggressive features of OCCCs.

Importantly, suppression of HNF-1β expression by siRNA promoted an increase in apoptosis in TOV-21G cells, consistent with an earlier report,[28] whereas Hec251 cells stably overexpressing HNF-1β treated with doxorubicin showed a decrease in the amount of apoptotic cells, along with increased bcl-2 expression. Moreover, transfection of

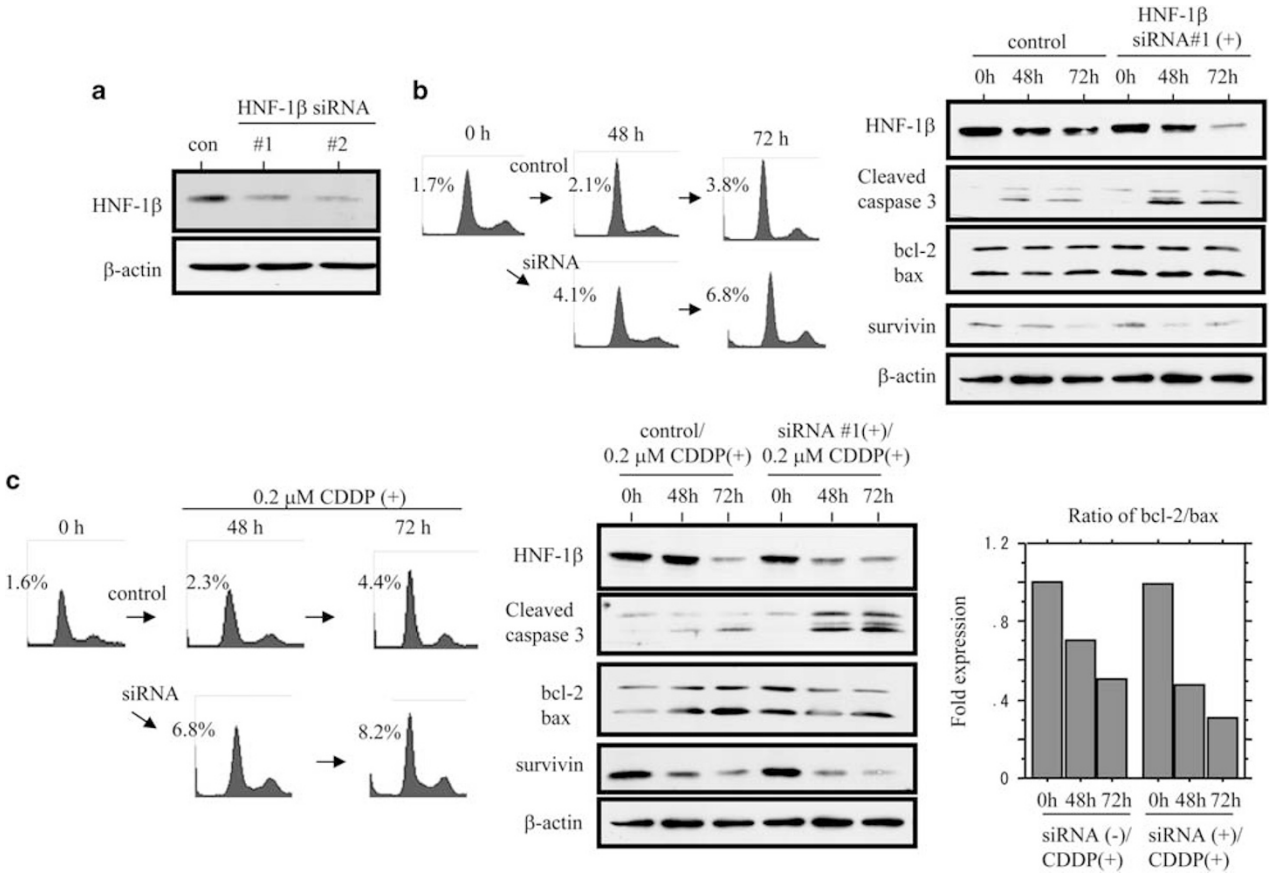

Figure 6 Inhibition of apoptosis by HNF-1*β*. (**a**) Suppression of endogenous HNF-1*β* expression by transfection of two siRNAs (#1 and #2) in TOV-21G cells. (**b**) Left: after transfection of siRNA#1 for HNF-1*β* into TOV-21G cells for the time shown, cells undergoing apoptosis (sub-G1) were detected by flow cytometry. These experiments were performed in triplicate, using independent samples. Right: analysis of protein expression levels by western blot assay in TOV-21G cells after transfection of HNF-1*β* siRNA for the time shown. (**c**) Left: after treatment of TOV-21G cells with or without transfection of siRNA#1 for HNF-1*β* with 0.2 *μ*M cisplatin (CDDP) for the time shown, cells undergoing apoptosis (sub-G1) were detected by flow cytometry. These experiments were performed in triplicate, using independent samples. Middle: analysis of protein expression levels by western blot assay in the TOV-21G cells with or without transfection of siRNA#1 for HNF-1*β* after treatment with 0.2 *μ*M CDDP for the time shown. Right: values of endogenous bcl-2 relative to bax protein in the TOV-21G cells with or without transfection of siRNA#1 for HNF-1*β* after treatment with 0.2 *μ*M CDDP were calculated by normalization to *β*-actin using the NIH ImageJ software. Expression level in the absence of transfection (0 h) is set as 1.

HNF-1*β* induced transcriptional upregulation of bcl-2 expression, in line with the IHC findings that demonstrated a positive correlation between the two in OCCCs. Given that toxic insults cause activation of the intrinsic apoptotic pathway through changes in expression of bcl-2 in the mitochondria,[29] it is suggested that HNF-1*β* may participate in blockade of mitochondrial-mediated (intrinsic) apoptotic events, leading to alteration in bcl-2 expression.

Although both HNF-1*β* score and amount of apoptotic cells were significantly higher in OCCCs with NG1 and non-solid growth pattern, evidence that supports a direct association between the two factors is lacking. In general, ovarian carcinomas accompanied by endometriosis show relatively higher level of 8-hydroxy-2′-deoxyguanosine (8-OHdG), which indicates severe oxidative DNA damage,[15] in line with our results demonstrating that pp65 scores were significantly higher in OCCCs as compared with the other subtypes of ovarian carcinomas. Given that the extrinsic apoptotic pathway is activated by cell death receptors, such as TNF-*α* receptors,[30,31] it is suggested that both extrinsic and intrinsic apoptotic pathways may be activated in OCCCs. With regard to overexpression of exogenous HNF-1*β* by treatment of the stable cells with doxorubicin, it appeared that toxic insults may also contribute to the regulation. Further studies to clarify these results are warranted.

In this study, an unexpected finding was that transfection of HNF-1*β* was able to increase transcription of the *Glut-1* gene, in line with a previous study,[27] but such an association was not observed in OCCCs. This may be owing to the presence of abundant and intricate signals that regulate glycolytic metabolism, such as HIF-1*α* pathways.[32]

Further, the lack of association between HNF-1β and HNF-4α expression in OCCCs was also unexpected because HNF-4α is one of the target genes of HNF-1β. Given our results that showed significantly higher HNF-4α expression in mucinous carcinomas, as well as OCCCs with aggressive features, it appeared that HNF-4α may have an important role in the establishment and maintenance of phenotypic characteristics in a subset of ovarian carcinomas.

In conclusion, our observations clearly define some of the functional roles of HNF-1β in OCCCs. Activation of NF-κB signaling and several apoptotic (cytotoxic) signals by several microenvironmental factors may cause transactivation of the *HNF-1β* gene. Subsequently, its overexpression may participate in cell survival by alteration of apoptotic events, particularly in mitochondria-mediated pathways, through upregulation of bcl-2 expression in OCCCs (Figure 8).

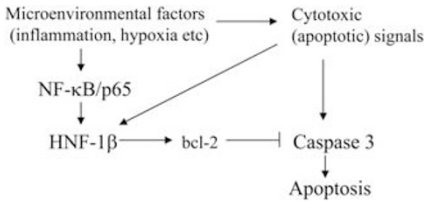

Figure 8 Schematic representation of associations among HNF-1β, NF-κB, and bcl-2 in response to microenvironment factors in ovarian clear cell carcinoma (OCCC) cells.

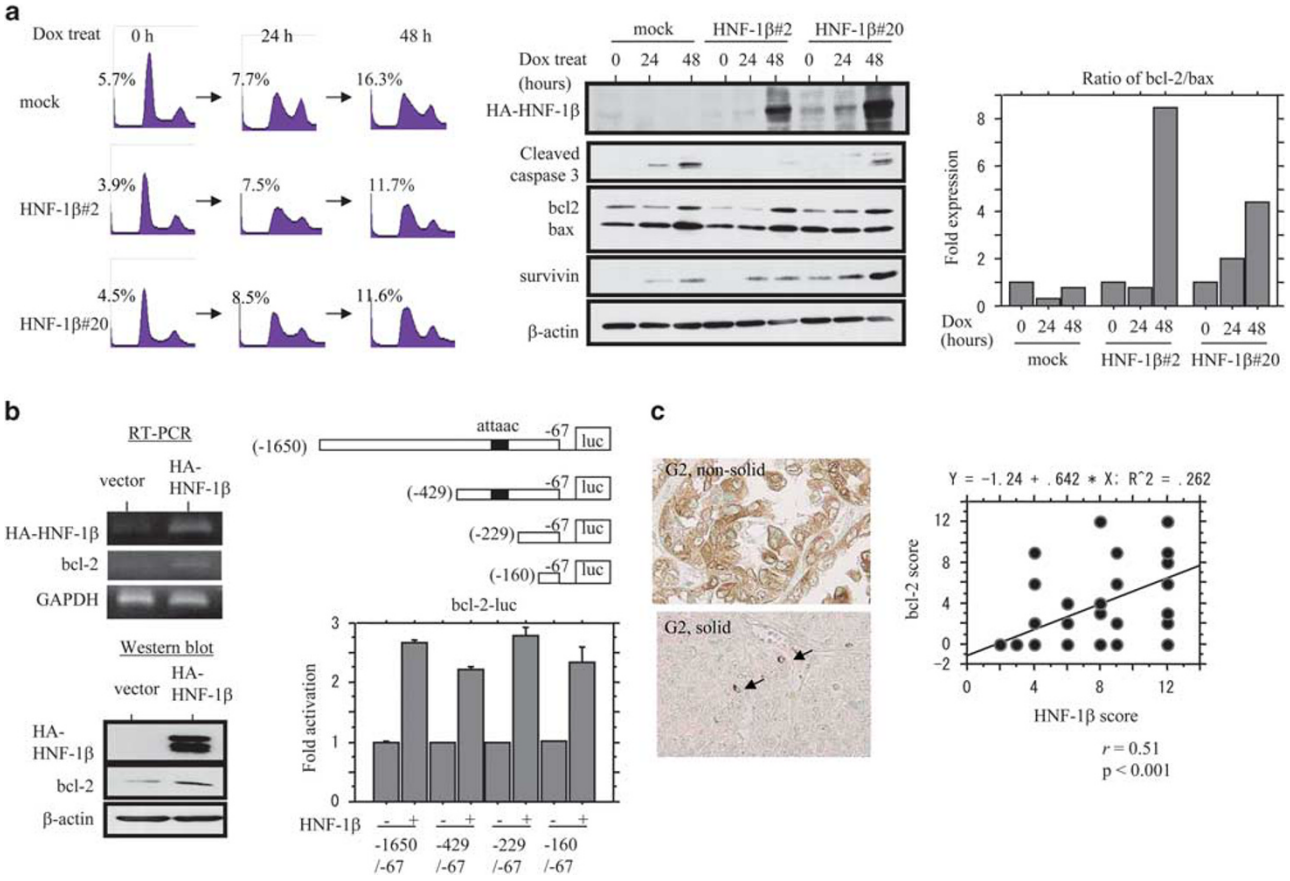

Figure 7 Transcriptional upregulation of *bcl-2* by HNF-1β. (**a**) Left: after treatment of two independent Hec251 cell lines stably overexpressing exogenous HA-HNF-1β with 1 μg/ml doxorubicin (Dox) for the time shown, cells undergoing apoptosis (sub-G1) were detected by flow cytometry. These experiments were performed in triplicate, using independent samples. Middle: analysis of protein expression levels by western blot assay in the two stable cell lines after treatment with 1 μg/ml doxorubicin for the time shown. HA-HNF-1β protein was detected by an anti-HA antibody. Right: values of endogenous bcl-2 relative to bax protein after treatment with 1 μg/ml doxorubicin were calculated by normalization to β-actin, using the NIH ImageJ software. Expression level in the absence of transfection (0 h) is set as 1. (**b**) Left: analyses of mRNA and protein expression levels of *bcl-2* using total RNA or protein extracted from HA-HNF-1β-transfected TOV-21G cells by reverse transcription PCR (RT-PCR; left) and western blot (right) assays, respectively. HA-HNF-1β mRNA was detected using a combination of HA-5′ forward (5′-TACCCATACGATGTTCCAGATTACGC-3′) and HNF-1β (388) reverse primers (Table 1), while HA-HNF-1β protein was detected by an anti-HA antibody. Right upper: various *bcl-2* promoter constructs were used for evaluating the transcriptional regulation by HNF-1β. Note the putative HNF-1β-binding site (5′-ATTAAC-3′). Right lower: TOV-21G cells were transfected with various constructs of the *bcl-2* promoter, along with the HNF-1β expression plasmid. The experiment was performed in triplicate. (**c**) Left: staining is by IHC for bcl-2 in ovarian clear cell carcinomas (OCCCs). Note the lack of bcl-2 immunoreactivity in OCCCs with solid features, in contrast to the bcl-2-positive infiltrating lymphocytes (indicated by arrows). Right: relationship between HNF-1β and bcl-2 scores in OCCCs.

Supplementary Information accompanies the paper on the Laboratory Investigation website (http://www.laboratoryinvestigation.org)

ACKNOWLEDGMENTS

This study was supported by a grant from JSPS KAKENHI Grand Number 25670179.

DISCLOSURE/CONFLICT OF INTEREST

The authors declare no conflicts of interest.

1. Anglesio MS, Carey MS, Kobel M *et al.* Clear cell symposium speaker: clear cell carcinoma of the ovary: a report from the first Ovarian Clear Cell Symposium, June 24 th, 2010. Gynecol Oncol 2011;121: 407–415.
2. Skirnisdottir I, Seidal T, Karlsson MG *et al.* Clinical and biological characteristics of clear cell carcinoma of the ovary in FIGO stages I-II. Int J Oncol 2005;26:177–183.
3. Sugiyama T, Kamura T, Kigawa J *et al.* Clinical characteristics of clear cell carcinoma of the ovary: a distinct histologic type with poor prognosis and resistance to platinum-based chemotherapy. Cancer 2000;88:2584–2589.
4. Chan JK, Teoh D, Hu JM *et al.* Do clear cell ovarian carcinoma have poorer prognosis compared to other epithelial types? A study of 1411 clear cell ovarian cancers. Gynecol Oncol 2008;109:370–376.
5. Itamochi H, Kigawa J, Toyota N.. Mechanisms of chemoresistance and poor prognosis in ovarian clear cell carcinoma. Cancer Sci 2008;99: 653–658.
6. Somigliana E, Vigano P, Parazzini F *et al.* Association between endometriosis and cancer: a comprehensive review and a critical analysis of clinical and epidemiological evidence [review]. Gynecol Oncol 2006;101:331–341.
7. Kobayashi H, Sumimoto K, Moniwa N *et al.* Risk of developing ovarian cancer among women with ovarian endometria: a cohort study in Shizuoka, Japan. Int J Gynecol Cancer 2007;17:37–43.
8. Bach I, Mattei MG, Cereghini S *et al.* Two members of an HNF1 homeoprotein family are expressed in human liver. Nucleic Acids Res 1991;19:3553–3559.
9. Parviz F, Matullo C, Garrison WD *et al.* Hepatocyte nuclear factor 4alpha controls the development of a hepatic epithelium and liver morphogenesis. Nat Genet 2003;34:292–296.
10. Lee YH, Sauer B, Gonzalez FJ.. Laron dwarfism and non-insulin-dependent diabetes mellitus in the Hnf-1alpha knock mouse. Mol Cell Biol 1998;18:3059–3068.
11. Kajihara H, Yamada Y, Kanayama S *et al.* Clear cell carcinoma of the ovary: potential pathogenic mechanism (review). Oncol Rep 2010;23: 1193–1203.
12. Kato N, Tamura G, Motoyama T. Hypomethylation of *hepatocyte nuclear factor-1beta (HNF-1beta)* CpG island in clear cell carcinoma of the ovary. Virchows Arch 2008;452:175–180.
13. Terasawa K, Toyota M, Sagae S *et al.* Epigenetic inactivation of *TCF2* in ovarian cancer and various cancer cell line. Br J Cancer 2006;94: 914–921.
14. Yamaguchi K, Mandai M, Oura T *et al.* Identification of an ovarian clear cell carcinoma gene signature that reflects inherent disease biology and the carcinogenic processes. Oncogene 2010;29:1741–1752.
15. Yamaguchi K, Mandai M, Toyokuni S *et al.* Contents of endometriotic cysts, especially the high concentration of free iron, are a possible cause of carcinogenesis in the cysts through the iron-induced persistent oxidative stress. Clin Cancer Res 2008;14:32–40.
16. Yamada Y, Shigetomi H, Onogi A *et al.* Redox-active iron-induced oxidative stress in the pathogenesis of clear cell carcinoma of the ovary. Int J Gynecol Cancer 2011;21:1200–1207.
17. Shigetomi H, Higashiura Y, Kajihara H *et al.* A potential link of oxidative stress and cell cycle regulation for development of endometriosis. Gynecol Endocrinol 2012;28:897–902.
18. Benedet JL, Bender H, Jones 3rd H *et al.* FIGO staging classifications and clinical practice guidelines in the management of gynecologic cancers. FIGO Committee on Gynecologic Oncology. Int J Gynaecol Obstet 2000;70:209–262.
19. Veras E, Mao T-L, Ayhan A *et al.* Cystic and adenofibromatous clear cell carcinomas of the ovary: distinctive tumors that differ in their pathogenesis and behavior: a clinicopathologic analysis of 122 cases. Am J Surg Pathol 2009;33:844–853.
20. Saegusa M, Hashimura M, Kuwata T *et al.* Requirement of the Akt/β-catenin pathway for uterine carcinosarcoma genesis, modulating E-cadherin expression through the transactivation of *slug*. Am J Pathol 2009;174:2107–2115.
21. Saegusa M, Hashimura M, Suzuki E *et al.* Transcriptional up-regulation of Sox9 by NF-κB in endometrial carcinoma cells, modulating cell proliferation through alteration in the $p14^{ARF}$/p53/$p21^{WAF1}$ pathway. Am J Pathol 2012;181:684–692.
22. Kerr JF, Winterford CM, Harmon BV.. Apoptosis: its significance in cancer and cancer therapy. Cancer 1994;73:2013–2026.
23. Tazo Y, Hara A, Onda T *et al.* Bifunctional roles of survivin-ΔEx3 and survivin-2B for susceptibility to apoptosis in endometrial carcinomas. J Cancer Res Clin Oncol 2014;140:2027–2037.
24. Schmidt KN, Amstad P, Cerutti P *et al.* The roles of hydrogen peroxide and superoxide as messengers in the activation of transcription factor NF-κB. Chem Biol 1995;2:13–22.
25. Bonello S, Zahringer C, BelAiba RS *et al.* Reactive oxygen species activate the HIF-1α promoter via a functional NF-κB site. Arterioscler Thromb Vasc Biol 2007;27:755–761.
26. Yoshida T, Hashimura M, Matsumoto T *et al.* Transcriptional upregulation of HIF-1α by NF-κB/p65 and its associations with β-catenin/p300 complexes in endometrial carcinoma cells. Lab Invest 2013;93: 1184–1193.
27. Okamoto T, Mandai M, Matsumura N *et al.* Hepatocyte nuclear factor-1β (HNF-1β) promotes glucose uptake and glycolytic activity in ovarian clear cell carcinoma. Mol Carcinog 2013;54:35–49.
28. Tsuchiya A, Sakamoto M, Yasuda J *et al.* Expression profile in ovarian clear cell carcinoma: identification of hepatocyte nuclear factor-1β as a molecular marker and a possible molecular target for therapy of ovarian clear cell carcinoma. Am J Pathol 2003;163:2503–2512.
29. Ling X, Cheng Q, Black JD *et al.* Forced expression of survivin-2B abrogates mitotic cells and induces mitochondria-dependent apoptosis by blockade of tubulin polymerization and modulation of bcl-2, bax, and survivin. J Biol Chem 2007;282:27204–27214.
30. Kelly RJ, Lopez-Chavez A, Citrin D *et al.* Impacting tumor cell-fate by targeting the inhibitor of apoptosis protein survivin. Mol Cancer 2011;10:35.
31. Miura K, Fujibuchi W, Unno M. Splicing variants in apoptotic pathway. Exp Oncol 2012;34:212–217.
32. Chen C, Pore N, Behrooz A *et al.* Regulation of *glut 1* mRNA by hypoxia-inducible factor-1. J Biol Chem 2012;276:9519–9525.
33. Tanaka T, Tomaru Y, Nomura Y *et al.* Comprehensive search for HNF-1beta-regulated genes in mouse hepatoma cells perturbed by transcription regulatory factor-targeted Rania. Nucleic Acids Res 2004;32:2740–2750.
34. Rebouissou S, Vasiliu V, Thomas C *et al.* Germline hepatocyte nuclear factor 1 alpha and 1 beta mutations in renal cell carcinomas. Hum Mol Genet 2005;14:603–614.